ACS APPLIED NANO MATERIALS

Article

www.acsanm.org

Composites Composed of Polydopamine Nanoparticles, Graphene Oxide, and ε-Poly-L-lysine for Removal of Waterborne Contaminants and Eradication of Superbugs

Avijit Pramanik,[†] Kaelin Gates,[†] Ye Gao,[†] Qinku Zhang,[†] Fengxiang X. Han,[†] Salma Begum,[†] Chris Rightsell,[‡] Dhiraj Sardar,[‡] and Paresh Chandra Ray*[,†]

[†]Department of Chemistry and Biochemistry, Jackson State University, Jackson, Mississippi 39217, United States

[‡]Department of Physics and Astronomy, University of Texas at San Antonio, San Antonio, Texas 78249, United States

Supporting Information

ABSTRACT: The World Health Organization (WHO) estimates that 30% people in the world lack access to safe drinking water due to the presence of toxic waterborne contaminants, which kills more than 7.6 million children every year. Marine mussels secure themselves in the environment via foot proteins containing 3,4-dihydroxy-L-phenylalanine (DOPA) and lysine amino acids. Inspired by mussel surface chemistry, in the current paper, we report the development of novel composite nanoparticles via functionalization of polydopamine nanoparticle with graphene oxide and ε-poly-L-lysine, which can be used in decontamination of toxic waterborne contaminants and disinfection of drug resistance pathogens from environmental water samples. Reported composite nanoparticles with specific surface area 410 m^2g^{-1}, pore volume 0.620 cm^3 g^{-1}, and pore size between 2 and 130 nm have been used as channels for water passage and captured toxic metals as well as drug resistant pathogens. The surface oxygen-containing groups from GO and the functional groups of catechols and amines in PD nanoparticles have been used as active sites for decontamination of heavy metals ions. ε-Poly-L-lysine, a natural antimicrobial peptide, has been attached to the composite nanoparticle for killing of superbugs captured by the membrane. Reported data demonstrated that composite nanoparticles can be used for efficient separation of several heavy toxic metals such as Cr^{6}+, Pb^{2+}, Cu^{2+}, Hg^{2+}, and Zn^{2+} from environmental water samples. The same membrane also can be used for 100% separation and eradication of different superbugs such as β-lactamase (ESBL)-producing *Klebsiella pneumoniae* (KPN) and methicillin-resistant *Staphylococcus aureus* (MRSA). Possible mechanisms for water contaminant separation and disinfection of superbugs using composite nanoparticles are discussed.

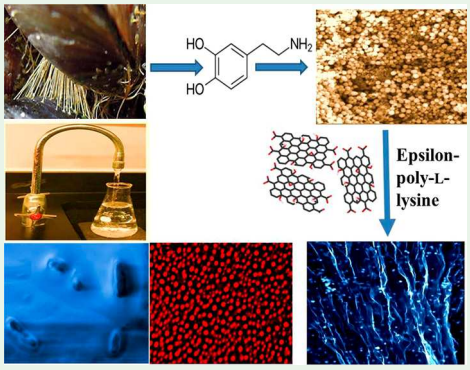

KEYWORDS: *polydopamine nanoparticles, graphene oxide, ε-poly-L-lysine, waterborne contamination, eradication of multidrug-resistant superbugs*

1. INTRODUCTION

According to the World Health Organization (WHO) and the United Nations (UN), 3 in 10 people in the world lack access to safe drinking water due to toxic waterborne pollutant infection.[1,2] Due to agricultural, medical, and other industrial pollutants contamination, common water sources are infected by heavy toxic metals such as As^{3+}, Pb^{2+}, Cu^{2+}, Hg^{2+}, and Zn^{2}, which raised huge concerns in our society for potential hazardous impacts on health.[1−4] As per UNICEF data published in 2018, waterborne diseases due to pathogenic bacteria infection in drinking water kill more than 7.6 million children every year in our society.[5−7] According to the Centers for Disease Control and Prevention (CDC) data published in 2018,[5−7] multidrug-resistant superbugs such as methicillin-resistant *Staphylococcus aureus* (MRSA) and β-lactamase (ESBL)-producing *Klebsiella pneumoniae* (KPN) are responsible for more than 2 million hospital-acquired infections and around 100,000 deaths annually.[5−7] Driven by the continuous rise of toxic metal concentrations in water and the number of new types of superbug strains in our society, there is an urgent demand for the search for new types of water separation membranes for the decontamination and disinfection of waterborne pollutants.[1−13] Here we report the design of mussels inspired surface chemistry based polydopamine nanoparticle (PD-NP) attached graphene oxide (GO) conjugated ε-poly-L-lysine (ε-PL) based composite nanoparticles, as shown in Scheme 1, which has capability for decontamination of toxic waterborne pollutants and disinfection of superbugs from environmental water samples.

Over billions of years of evolution, nature has optimized materials with unique combinations of functions to achieve maximal performance in this environment.[14−20] For example, marine mussels are well-known to be the masters of adhesion

Received: January 25, 2019
Accepted: April 8, 2019
Published: April 15, 2019

DOI: 10.1021/acsanm.9b00161
ACS Appl. Nano Mater. XXXX, XXX, XXX−XXX

Scheme 1[a]

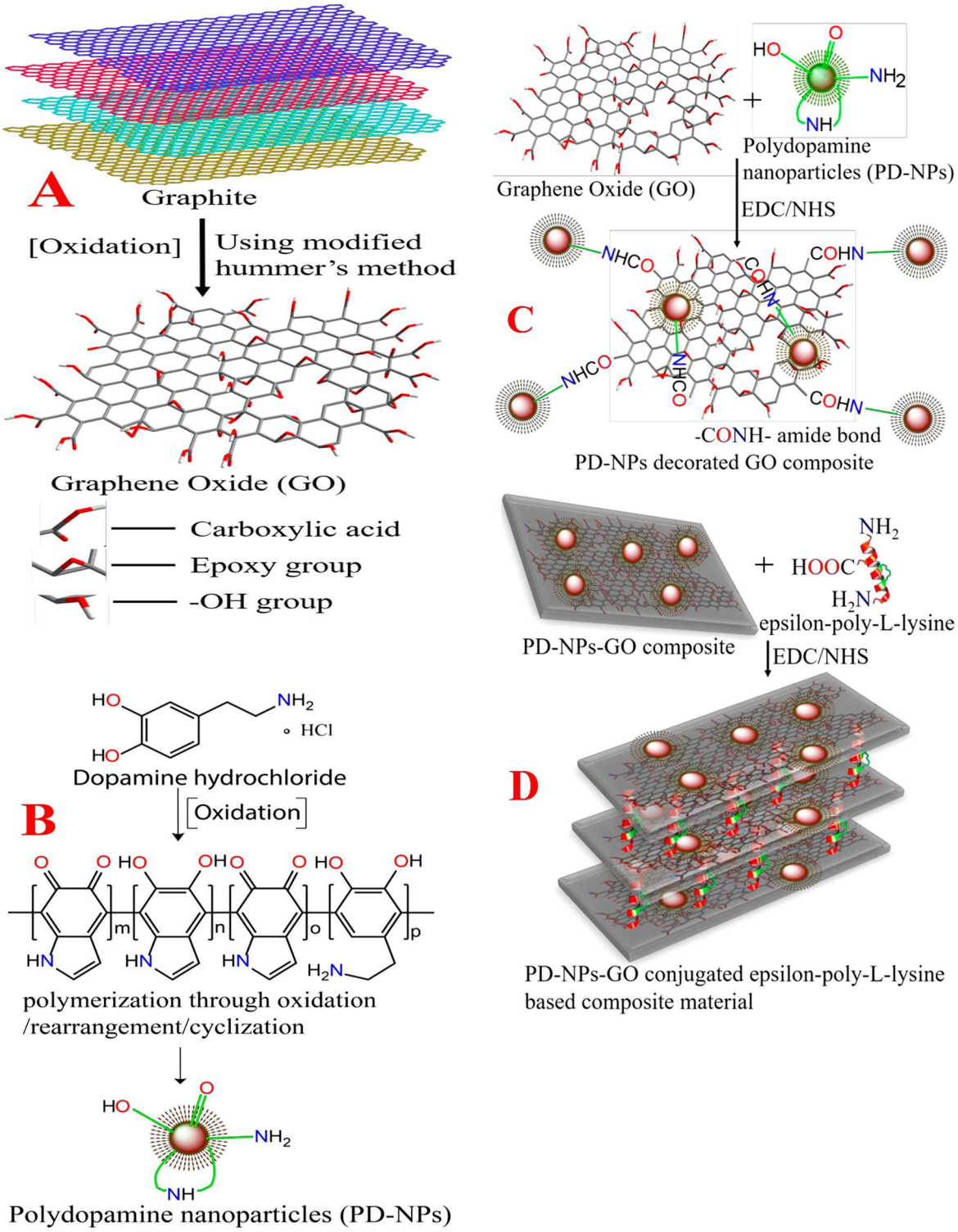

[a](A) Development of graphene oxide from graphite using Hummer's method. (B) Development of polydopamine nanoparticle from polydopamine via polymerization. (C) Synthetic procedures we have used to develop PD-NP attached two dimensional GO. (D) Synthetic procedures we have used to develop PD-NP attached GO conjugated ε-PL based three-dimensional composite nanoparticle.

due to the presence of *Mytilus edulis* foot protein-5, which contain 3,4-dihydroxy-L-phenylalanine (DOPA) and lysine (Lys).[20−28] At the molecular level, catechol from DOPA and amine from lysine in the *Mytilus edulis* foot protein are believed to be highly crucial for achieving strong adhesion properties.[20−28] Catecholamines including dopamine are well documented to be considered as small-molecule mimics of the adhesive proteins of mussels.[14−20] Due to the widespread use of mussel-inspired surface chemistry using dopamine and lysine,[20−28] we have reported the design of a PD-NP attached GO conjugated ε-PL based composite nanoparticle which shows promise as a versatile platform for the separation of toxic

DOI: 10.1021/acsanm.9b00161
ACS Appl. Nano Mater. XXXX, XXX, XXX−XXX

waterborne pollutants like heavy metals and superbugs, as well as disinfection of superbugs.

Graphene oxide (GO), developed via strong oxidation of graphene, contains a huge amount of oxygen-containing functional groups such as hydroxyl, carboxyl, and epoxy, on both basal planes and edges.[29−40]

In the last few years, we and other groups have reported that GO is highly useful for the development of two-dimensional (2D) and three-dimensional (3D) composites with significant potential for broad use in water purification applications.[34−42] In our design, the surface oxygen-containing groups from GO in the membrane allow removal of positively charged heavy metal irons via electrostatic interaction, In the reported three-dimensional composite nanoparticle, dopamine plays multi-functional roles and those are the formation of polydopamine (PD) nanoparticles from dopamine hydrochloride in the presence of tris buffer as well as surface functionalization agents for graphene oxides to develop composite nanoparticles with plenty of interconnected pores with pore size between 2 and 130 nm, which has been used as channels for water passage. Since the surfaces of PD nanoparticles have abundant functional groups of catechols and amines, in our design, those surface functional groups have been used as active sites for decontamination of water via interaction with heavy metal ions. Since the sizes of superbugs are 1 μm and above whereas the pore size of the membrane is below 300 nm, all superbugs are captured by the membrane, because superbugs are not able to pass through the membrane. We have used ε-poly-L-lysine, a natural antimicrobial peptide,[43−45] for killing of superbugs captured by the membrane. Since ε-poly-L-lysine is known to kill micro-organisms via disruption of a cell membrane, it has been used as food preservative in industry very often.[43−45] In our design, for the disinfection of superbugs we have developed ε-poly-L-lysine attached PD nanoparticle conjugated composite nano-particle, as shown in Scheme 1. Reported data in the paper shows that ε-poly-L-lysine attached PD nanoparticle conjugated composite nanoparticles can be used for efficient separation of several waterborne toxic metals such as Cr^{6+}, Pb^{2+}, Cu^{2+}, Hg^{2+}, Cr^{3+}, and Zn^{2+} from environmental water samples from different sources. We have also demonstrated that the same architecture can be used for 100% separation and eradication of different super bugs such as MRSA and ESBL-KPN from environmental water samples from different sources.

2. RESULTS AND DISCUSSION

2.1. Design of Novel Composite Nanoparticle via Functionalization of Polydopamine with Graphene Oxide and ε-Poly-L-lysine. As shown in Scheme 1, we used a multistep synthetic procedure to develop PD-NP attached GO conjugated ε-PL based composite nanoparticles. As reported in Scheme 1A, initially we developed water-soluble graphene oxide from graphite using the well documented Hummer's method as we and others have reported before.[29−40] After that, we developed polydopamine nanoparticles, as reported in Scheme 1B. PD-NPs were synthesized using the following literature procedure via a modified Stöber method.[20−28] For this purpose, 1.0 g of dopamine hydrochloride was dissolved in a solution of 100 mL of ethyl alcohol and 200 mL of water. Subsequently, 4 mL of concentrated NH_4OH was finally added to the reaction mixture under vigorous stirring at room temperature. After 24 h, PD-NPs were separated via centrifugation at 8500, washed with water several times, and dried under vacuum. As shown in Scheme 1C, in the next step, we developed PD-NP-graphene

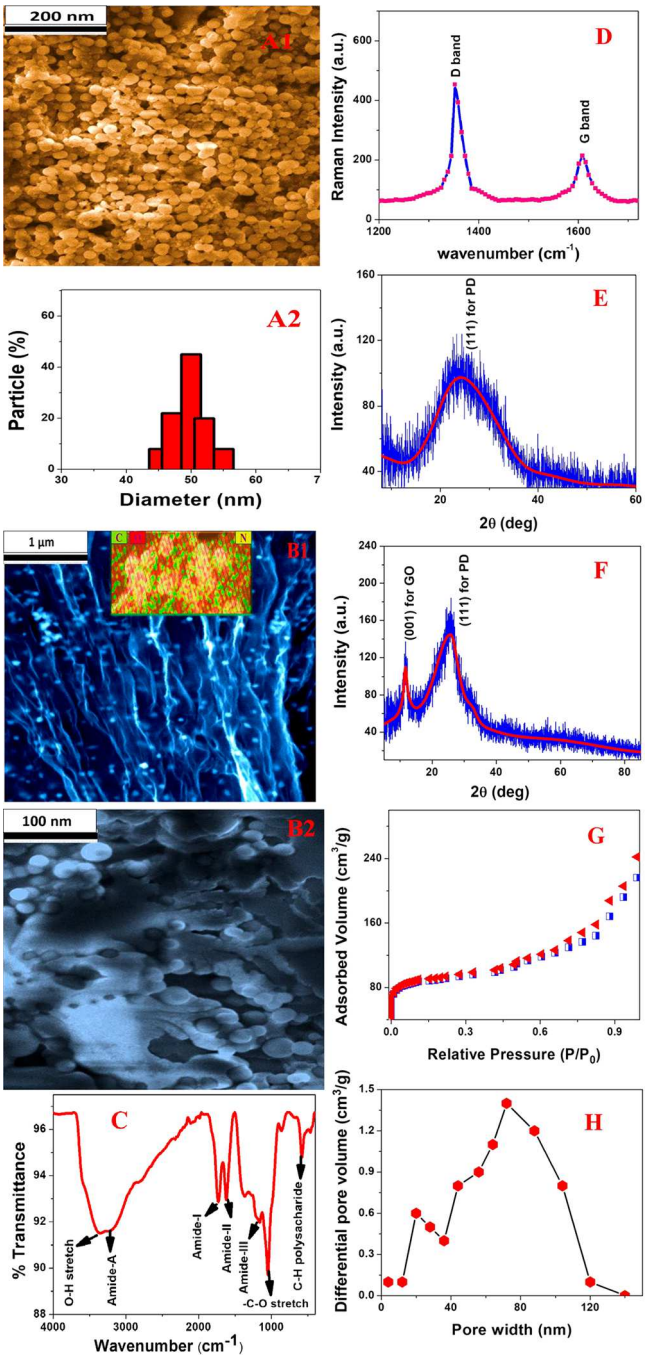

Figure 1. (A1) Surface SEM image of polydopamine nanoparticle developed via a modified Stöber method. SEM image shows the particle size is 50 ± 6 nm. (A2) SEM analysis shows the percent of different size polydopamine particles, which indicates that the particle size varies from 44 to 56 nm. (B1, B2) SEM images from PD-NP attached GO conjugated ε-PL based composite nanoparticle: (B1) surface view and (B2) cross section view. Insert EDX data in B1 show the presence of C, N, and O. (C) FTIR spectra of PD-NP attached GO conjugated ε-PL based composite nanoparticle, which shows the presence of −OH stretch, amide-A, amide-I, amide-II, amide-III, and −CO stretch and −C−H polysaccharide vibrational bands. (D) Raman spectra from PD-NP attached GO conjugated ε-PL based composite nanoparticle indicates the presence of D and G bands. (E) X-ray diffraction spectra from PD-NP indicate the presence of (111) reflection for polydopamine. (F) X-ray diffraction spectra from composite nanoparticle, which indicate the presence of (111) reflection for polydopamine and (001) reflection for GO. (G) N_2 adsorption/desorption isotherm of

DOI: 10.1021/acsanm.9b00161
ACS Appl. Nano Mater. XXXX, XXX, XXX−XXX

Figure 1. continued

PD-NP attached GO conjugated ε-PL based composite nanoparticle, which shows type III isotherms. (H) Pore size distributions from PD-NP attached GO conjugated ε-PL based composite nanoparticle, which shows pore size ranging from 2 to 130 nm and highest density at around 70 nm.

oxide based composite nanoparticles. For this purpose, 200 mg of freeze-dried graphene oxide (GO) was dispersed in 250 mL of double distilled water through ultrasonication for 2 h. To this suspension, dopamine nanoparticles were added and stirred. Then we used EDC (1-ethyl-3-(3-(dimethylamino)propyl)-carbodiimide)/NHS (*N*-hydroxysuccinimide) chemistry to develop dopamine nanoparticle attached GO. In the next step, ε-poly-L-lysine was added to the dopamine nanoparticle attached GO, as shown in Scheme 1D. After that we used EDC coupling chemistry to develop composite nanoparticles. Then the mixture was sonicated for 30 min. In the next step, we kept the sample mixture on an oil bath at about 80 °C under a hood for 90 min.

After that, we performed sonication for 1.5 h to separate PD-NP attached GO conjugated ε-PL based composite nanoparticle from the reactants. After sonication, the semisolid product was used to develop the round shape membrane using spin-casting at 1500 rpm onto the glass substrate. Finally, we performed vacuum-drying overnight at 60 °C. After that, the PD-NP attached GO conjugated ε-PL based composite nanoparticle membrane was removed from the glass substrate and stored for use for water purification.

We used high-resolution tunneling electron microscopy (HRTEM), energy-dispersive X-ray (EDX) spectroscopy, X-ray diffraction (XRD) spectroscopy, Raman spectroscopy, and other techniques as we have reported before,[11−13,36−39] to characterize PD nanoparticle and PD-NP attached GO conjugated ε-PL based composite nanoparticles. Scanning electron microscopy (SEM) image, as reported in Figure 1A1, and SEM image analysis as reported in Figure 1A2 show that the average size for freshly developed polydopamine nanoparticle via modified Stöber method is 50 ± 6 nm. Similarly, the SEM image, as reported in Figure 1B1 and B2, shows the morphology of freshly developed PD-NP attached GO conjugated ε-PL based porous architecture. The inset EDX data clearly shows the presence of C, N, and O in our developed composite nanoparticles. As reported in Figure 1C, the Fourier transform infrared (FT-IR) spectroscopy of our developed composite nanoparticle, shows the presence several different types of surface functional groups such as amide A, −OH, amide-I, amide-II, amide-III, and C═O. The presence of different amide groups indicates that graphene oxides are attached with peptide and polydopamine nanoparticles. The Raman spectra from composite nanoparticles, as reported in Figure 1D, clearly shows the presence of D and G bands which originate from graphene oxide.[29−40] Figure 1E shows the powder XRD spectrum of polydopamine nanoparticles, which indicates the presence of (111) reflection for polydopamine.[20−26] On the other hand, XRD data from composite nanoparticles, as reported in Figure 1F, shows two peaks and those are the (111) reflection for polydopamine and (001) reflection for GO.[20−28]

We measured the specific surface area for freshly developed PD-NP attached GO conjugated ε-PL based composite nanoparticles using N_2 adsorption/desorption data. For this purpose, we used a Tristar II 3020 surface area analyzer (Micromeritics). Experimental details have been reported previously.[36,39] On the other hand, for the measurement of pore size distribution for freshly developed PD-NP attached GO conjugated ε-PL based composite nanoparticles, we used the Barrett−Joyner−Halenda (BJH) method. Experimental details have been reported previously.[36,39] Brunauer−Emmett−Teller (BET) analysis from PD-NP attached GO conjugated ε-PL based composite nanoparticles, as reported in Figure 1G, indicates that the specific surface area for our developed architecture is 410 $m^2\ g^{-1}$, with a pore volume of 0.620 $cm^3\ g^{-1}$. Using the BJH method, we also estimated the pore size distribution, as reported in Figure 1H, which indicates that the pore size ranges from 2 to 130 nm. In the next step, we also measured the water flux for PD-NP attached GO conjugated ε-PL based composite nanoparticles. For this purpose, we collected the permeated water through the nanoporous composites using an electronic balance, as we have reported before.[36−39] From the experiment, we estimated the water flux for PD-NP attached GO conjugated ε-PL based composite nanoparticle to be 138.2 L $m^{-2}\ h^{-1}\ bar^{-1}$.

2.2. Use of PD-NP Attached GO Conjugated ε-PL Based Composite Nanoparticle for Decontamination of Toxic Metal from Environmental Water Sample. Next, to find out whether PD-NP attached GO conjugated ε-PL based composite nanoparticlse can be used for the decontamination of toxic metal from environmental water samples, we performed several different experiments as discussed below. At first, we infected the drinking water sample with Cr(VI), Hg(II), Pb(II), Cd(II), and Zn(II), selectively and simultaneously. For the selective toxic metal ion experiment, we used 10 ppm concentration of each toxic metal

For the mixture of all five metals ion experiment, we used 2 ppm concentration for each metal. After that, we performed filtration using our developed PD-NP attached GO conjugated ε-PL based composite nanoparticles. At the end, we used inductively coupled plasma mass spectrometry (ICP-MS) for determining the removal efficiency of different toxic metals using PD-NP attached GO conjugated ε-PL based composite nanoparticles. As shown in Figure 2A−D, the reported experimental data indicates that the removal efficiency for Cr(VI) is 89% and that for Hg(II) is 93%. Whereas the removal efficiency for Pb(II) is 95% and that for Cd(II) is 90%. The observed high removal efficiency using our developed PD-NP attached GO conjugated ε-PL based composite nanoparticles is due to the fact that polydopamine contains amine and catechol functionalities which are capable of scavenging metals. Also, in the presence of nitrogen heteroatoms, PD nanoparticles have a strong tendency to interact with positively charged metal ions, which also helps to remove toxic metal ions.[20−26] On the other hand, the surface oxygen-containing groups in graphene oxide allow removal of positively charged heavy metal ions via electrostatic interaction.[30−38] Since in real life a water sample can contain all different metal ions together, next we performed a filtration experiment where all five toxic metals are present in the water. As shown in Figure 2F, the toxic metal removal efficiency is between 80 and 90%, when several toxic metals are present together.

Next, to find out whether PD-NP attached GO conjugated ε-PL based composite nanoparticles can be used for the separation of toxic metals from an environmental sample, we used tap water, lake water, Mississippi River water, and Mississippi reservoir water samples spiked with Cr(VI), Hg(II), Pb(II), Cd(II), and Zn(II) (2 ppm concentration each) simultaneously.

DOI: 10.1021/acsanm.9b00161
ACS Appl. Nano Mater. XXXX, XXX, XXX−XXX

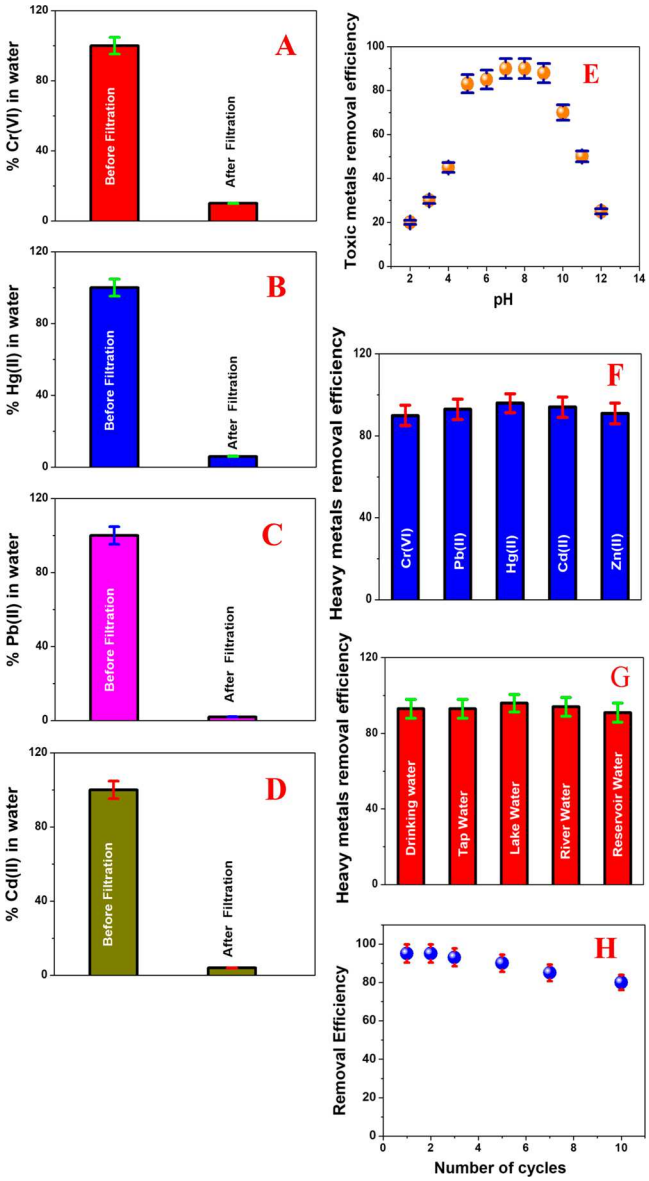

Figure 2. (A) Cr(VI) (10 ppm concentration) removal efficiency from drinking water using PD-NP attached GO conjugated ε-PL based composite nanoparticles. (B) Hg(II) (10 ppm concentration) removal efficiency from drinking water using PD-NP attached GO conjugated ε-PL based composite nanoparticles. (C) Pb(II) (10 ppm concentration) removal efficiency from drinking water using PD-NP attached GO conjugated ε-PL based composite nanoparticles. (D) Cd(II) (10 ppm concentration) removal efficiency from drinking water using PD-NP attached GO conjugated ε-PL based composite nanoparticles. (E) Plot showing how the pH of water influences the removal efficiency for a mixture of different toxic metals [Cr(VI), Hg(II), Pb(II), Cd(II), and Zn(II)] (2 ppm concentration for each metal ion) from drinking water using PD-NP attached GO conjugated ε-PL based composite nanoparticles. (F) Percentage of toxic metal removal efficiency for a mixture of different toxic metals [Cr(VI), Hg(II), Pb(II), Cd(II), and Zn(II)] (2 ppm concentration for each metal ion) from drinking water using PD-NP attached GO conjugated ε-PL based composite nanoparticles. (G) Plot showing how the source of water influences the toxic metal removal efficiency for a mixture of different toxic metals [Cr(VI), Hg(II), Pb(II), Cd(II), and Zn(II)] (2 ppm concentration for each metal ion) using PD-NP attached GO conjugated ε-PL based composite nanoparticles. (H) Plot showing how the removal efficiency of different toxic metals [Cr(VI), Hg(II), Pb(II), Cd(II), and Zn(II)] (2 ppm concentration for each metal ion) varies with number of cycles of filtration.

Since the pH can be different for different sources of water, initially we performed an experiment on how the pH of water can influence the removal efficiency of different toxic metal ions. As shown in Figure 2E, the best performance is observed when pH is between 5 and 9. At higher acidic and basic pH, the removal efficiency decreases and this is due to the fact the oxygen functional groups in GO and amine, catechol groups in PD is highly protonated in acidic pH and deprotonated in basic pH. Due to the observed pH effect, we measured the pH of environmental water collected from tap water, lake water, Mississippi River water, and Mississippi reservoir and we determined that the pH varies from 5 to 9. Experimental data reported in Figure 2G clearly shows that the toxic metal removal efficiency varies between 80 and 90%. The reported data also indicates that although environmental water from different sources contains different organic compounds and other metals ions like sodium, potassium, and magnesium, our developed PD-NP attached GO conjugated ε-PL based composite nanoparticles can be used for targeted metal ion separation in the presence of other metal ions and organic pollutants. As reported in Figure 1H, the removal efficiency performance for the composite material decreases around 10% after 10 cycles of filtration. The observed decrease in removal efficiency can be due to the fouling issue of composite material which occurs due to the accumulation of microorganisms on the surface from the environmental water sample. To compare the removal efficiency for the developed composite materials with a commercially available activated carbon filter, we also performed the same experiment with an activated carbon filter. From the experimental data, we found out that the removal efficiency for heavy metals using the developed composite material is comparable for the activated carbon filter. Although removal efficiency is comparable, we have noted the removal efficiency performance is almost unchanged after 10 cycles for the activated carbon filter, whereas as reported in Figure 2H the removal efficiency performance decreases around 10% after 10 cycles for the developed composed materials,

2.3. Use of Composite Nanoparticle for Disinfection of Superbugs from Environmental Water Sample. Next, to find out whether PD-NP attached GO conjugated ε-PL based composite nanoparticle can be used for the removal and killing of superbugs from environmental water samples, we performed several different experiments as discussed below. At first, we infected the drinking water sample with MRSA and KPN superbugs, selectively and simultaneously. For the selective separation and killing experiment, we used a 1×10^5 CFU/mL concentration of each superbug. For the mixture of MRSA and KPN superbugs experiment, we used a 5×10^4 CFU/mL concentration for each superbug. After that, we performed filtration using our developed PD-NP attached GO conjugated ε-PL based composite nanoparticles. At the end, we used reverse transcription polymerase chain reaction (RT-PCR) technique and colony plating technique on LB agar for determining the removal efficiency of different toxic metals using PD-NP attached GO conjugated ε-PL based composite nanoparticles. Experimental details have been reported previously.[11−13,36−39]

Colony counting data reported in Figure 3A,B and RT-PCR data reported in Figure 3D−F clearly show that almost 100% of

DOI: 10.1021/acsanm.9b00161
ACS Appl. Nano Mater. XXXX, XXX, XXX−XXX

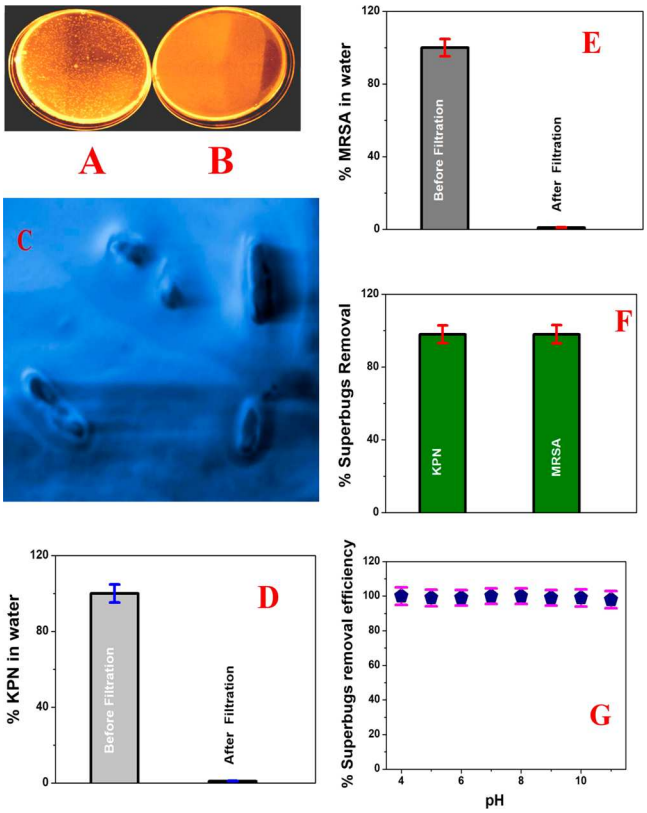

Figure 3. (A, B) Colony counting data shows colonies of KPN, which indicate the amount of live KPN superbugs (A) before filtration and (B) after filtration using PD-NP attached GO conjugated ε-PL based composite nanoparticles. (C) Top view SEM image data after filtration using PD-NP attached GO conjugated ε-PL based composite nanoparticles, which shows that KPN superbugs are captured by composite nanoparticle. membrane. (D) Plot showing the percentage of KPN removed using PD-NP attached GO conjugated ε-PL based composite nanoparticles, when the KPN concentration was 1×10^5 CFU/mL. (E) Plot showing the percentage of MRSA removed using PD-NP attached GO conjugated ε-PL based composite nanoparticles, when the MRSA concentration was 1×10^5 CFU/mL. (F) Percentage of superbug removal efficiency for the mixture of MRSA and KPN in water (5×10^4 CFU/mL concentration for each superbug) using PD-NP attached GO conjugated ε-PL based composite nanoparticles. (G) Plot showing how the pH of water influences the removal efficiency for a mixture of superbugs from drinking water using PD-NP attached GO conjugated ε-PL based composite nanoparticles.

KPN and MRSA can be removed selectively or simultaneously using our PD-NP attached GO conjugated ε-PL based 3D architecture. Our observed very high removal efficiency for KPN and MRSA using the PD-NP attached GO conjugated ε-PL based composite nanoparticles is due to the fact that the size of the superbugs is larger than the pore size of the composite nanoparticles. Since the size of KPN is greater than 1 μm and the size of MRSA is between 0.5 and 1 μm, whereas the pore size of our PD-NP attached GO conjugated ε-PL based composite nanoparticles is less than 120 nm, only water can pass through. On the other hand, due to the much bigger size, superbugs will not able to go through the PD-NP attached GO conjugated ε-PL based composite nanoparticles. To characterize the captured superbugs by our developed PD-NP attached GO conjugated ε-PL based composite nanoparticles, we performed a high-resolution SEM experiment as shown in Figure 3B. Reported experimental data clearly indicate that superbugs are captured on the surface of the membrane. Since the pH of water can be different for different sources of water, we also performed an experiment on how the pH of water can influence the removal efficiency of different superbugs. As shown in Figure 3G, the removal efficiency is almost independent of the pH of water within the range of 4−11. The observed almost pH independent superbug removal efficiency is mainly due to the fact that the superbugs are captured due to their size which is much larger than the pore size of our developed PD-NP attached GO conjugated ε-PL based composite nanoparticles. Since pH change can only change the protonation or deprotonation character for the functional groups attached with membrane and it does not effect the pore size abruptly, we did not observe any significant change in superbug removal efficiency as we vary the pH of water. Since superbugs like MRSA and KPN are known to be transmitted through contaminated water, for possible practical uses for our developed PD-NP attached GO conjugated ε-PL based composite nanoparticles, it is extremely important that the composite nanoparticles have the capability to disinfect superbugs after separation. To find out whether PD-NP attached GO conjugated ε-PL based composite nanoparticles can be used for the killing of superbugs which have been captured from environmental water samples, we performed several different experiments as discussed below. After filtration, we used the colony plating technique on LB agar as well as LIVE/DEAD BacLight Molecular Probes kit for determining the amounts of live/dead bacteria after capture by PD-NP attached GO conjugated ε-PL based composite nanoparticles. Experimental details for colony plating technique on LB agar as well as LIVE/DEAD BacLight Molecular Probes kit have been reported before.[11−13] As reported in Figure 4A−D, almost 100% of MRSA and KPN superbugs are killed when they are captured by our developed PD-NP attached GO conjugated ε-PL based composite nanoparticles.

Next to determine the superbug killing mechanism using our developed PD-NP attached GO conjugated ε-PL based composite nanoparticles, we also performed the same experiment with PD-NP attached GO based composite nanoparticles without ε-PL, As reported in Figure 3C, less than 20% KPN and MRSA superbugs are killed when those superbugs are captured by PD-NP attached GO based composite nanoparticles without ε-PL; on the other hand 100% KPN and MRSA superbugs are killed when those superbugs are captured by PD-NP attached GO conjugated ε-PL based composite nanoparticles. Around 18% superbug death using PD-NP attached GO based composite nanoparticles is due to the mechanical wrapping which may cause induced membrane stress, disrupting and damaging cell membranes, as we and others reported before.[36−39,41,42] Mechanical wrapping of KPN superbugs also can be seen in the SEM image reported as Figure 3C in this paper. Reported results in Figure 3C clearly indicate that attachment of ε-PL antimicrobial peptide in composite nanoparticles is very important for disinfection of superbugs. It is now well reported that ε-PL can bind to the membrane surface of bacteria by electrostatic interaction.[43−45] It is also well-known that ε-PL antimicrobial peptide can fracture the membrane surface of bacteria, and as a result the cell contents leak out.[43−45]

To understand whether our developed PD-NP attached GO conjugated ε-PL based composite nanoparticles can damage the membrane of superbugs, we performed a bacterial ATP leakage experiment using Molecular Probes ATP determination kit (Thermo Fisher Scientific). Experimental details have been

DOI: 10.1021/acsanm.9b00161
ACS Appl. Nano Mater. XXXX, XXX, XXX−XXX

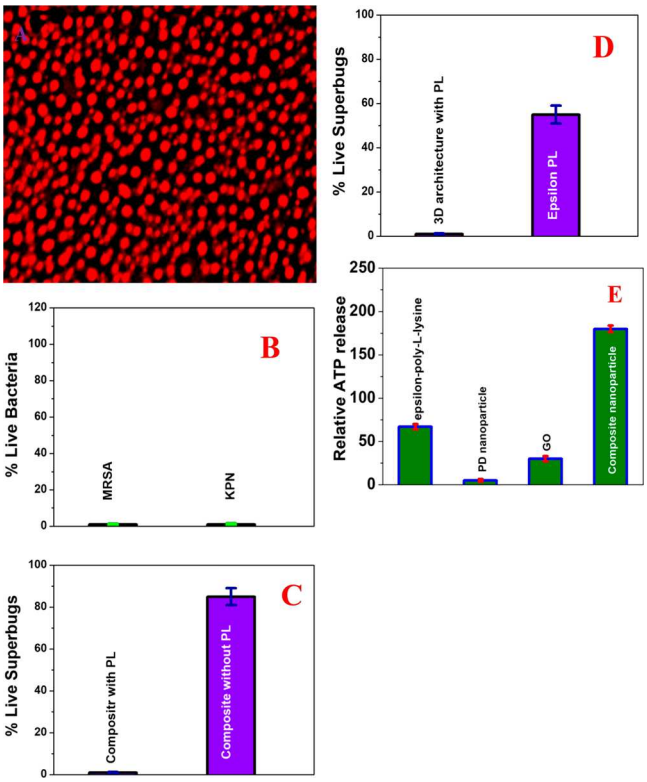

Figure 4. (A) MRSA superbug viability after filtration using PD-NP attached GO conjugated ε-PL based composite nanoparticles. We used the Molecular Probes LIVE/DEAD BacLight Bacterial Viability kits to determine amount of live and dead superbugs after filtration. (B) Plot indicating percentage of live MRSA and KPN superbugs after filtration using PD-NP attached GO conjugated ε-PL based composite nanoparticles. We used colony counting as well as Molecular Probes LIVE/DEAD BacLight Bacterial Viability kits to determine the amount of live and dead superbugs. (C) Plot indicating percentage of live KPN superbugs after filtration using PD-NP attached GO based composite nanoparticles without ε-PL and PD-NP attached GO conjugated ε-PL based composite nanoparticles. We used colony counting as well as Molecular Probes LIVE/DEAD BacLight Bacterial Viability kits to determine the amount of live and dead KPN superbugs. (D) Plot indicating percentage of live KPN superbugs when treated with ε-PL only and after filtration using PD-NP attached GO conjugated ε-PL based composite nanoparticles. We used colony counting as well as Molecular Probes LIVE/DEAD BacLight Bacterial Viability kits to determine the amount of live and dead KPN superbugs. (E) Plot showing relative cellular ATP leakage percentage for KPN superbugs when bacteria were treated with ε-PL, PD nanoparticles, GO and PD-NP attached GO conjugated ε-PL based composite nanoparticles separately.

reported before.[11,12] For this experiment, PEG coated gold nanoparticles, which are known to be nontoxic, are utilized, as we and others have reported before. ATP leakage experiment data as reported in Figure 4E clearly shows our developed PD-NP attached GO conjugated ε-PL based composite nanoparticles can promote high leakage of cellular ATP in the case KPN. Reported data also shows that ε-PL also promotes leakage of cellular ATP, but the amount is much lower than that caused by PD-NP attached GO conjugated ε-PL based composite nanoparticles. Experimental data reported in Figure 4D also indicate that only ε-PL can kill only 55% KPN when the concentration of ε-PL used was 100 μM. On the other hand, PD-NP attached GO conjugated ε-PL based composite nanoparticles can kill 100% KPN, although the concentration of ε-PL used was 100 μM for composite nanoparticle formation.

To understand the observed experimental data, we have determined the minimum inhibitory concentrations (MICs) for ε-PL against KPN and MRSA, using the National Committee for Clinical Laboratory Standards [NCCLS]. Experimental details have been reported before.[12] From the experimental results, the MICs of ε-PL were determined to be 220 μM for MRSA and 175 μM for KPN. The observed very high killing of superbugs using PD-NP attached GO conjugated ε-PL based composite nanoparticles can be due to the fact that when superbugs are trapped by composite nanoparticles, it causes high membrane stress. It becomes a very good condition for ε-PL to bind to the membrane surface of bacteria by electrostatic interaction and fracture the membrane surface of bacteria, and as a result superbugs are killed due to the disrupted and damaged cell membranes.

3. CONCLUSIONS

In the current Article, we have reported the development of PD-NP attached GO conjugated ε-PL based novel composite nanoparticles via functionalization of polydopamine nanoparticles with graphene oxide and ε-poly-L-lysine. Experimental data reported in this paper indicate that our developed PD-NP attached GO conjugated ε-PL based composite nanoparticles can be used in the decontamination of toxic waterborne contaminants and disinfection of drug resistant pathogens from environmental samples. We have shown that composite nanoparticles can be used for efficient separation of several heavy toxic metals such as Cr^{6}+, Pb^{2+}, Cu^{2+}, Hg^{2+}, and Zn^{2+} from environmental water samples. Reported data also shows that porous composites developed by us can be used for simultaneous removal of several toxic metals together from environmental river, lake, and tap water samples. We have also demonstrated that PD-NP attached GO conjugated ε-PL based composite nanoparticles can be used for 100% separation and eradication of different superbugs. Experimental data indicates that since the pore size of the PD-NP attached GO conjugated ε-PL based composite nanoparticles (less than 130 nm) is much smaller than the size of KPN and MRSA superbugs, 100% of superbugs were captured by the membrane and only water passed through the porous membrane. Reported superbug killing data shows that PD-NP attached GO conjugated ε-PL based composite nanoparticles not only captured the superbugs but also killed them totally. Although our reported data show that the developed novel composite nanoparticles may be used for the separation of toxic metals and disinfection of superbugs, research needs to be performed for proper engineering design to obtain highly repeatable and recyclable membranes for multiple end-use applications.

■ ASSOCIATED CONTENT

Supporting Information

The Supporting Information is available free of charge on the ACS Publications website at DOI: 10.1021/acsanm.9b00161.

Detailed synthesis, characterization of composite nanoparticles and other experiments(PDF)

■ AUTHOR INFORMATION

Corresponding Author

*E-mail: paresh.c.ray@jsums.edu. Fax: +16019793674

DOI: 10.1021/acsanm.9b00161
ACS Appl. Nano Mater. XXXX, XXX, XXX−XXX

ORCID

Paresh Chandra Ray: 0000-0001-5398-9930

Notes

The authors declare no competing financial interest.

■ ACKNOWLEDGMENTS

P.C.R. thanks NSF-PREM Grant # DMR-1205194, NSF CREST Grant # 1547754, and NSF-RII-EPSCoR Grant #1632899 for their generous funding. D.S. would like to acknowledge the support from UTSA through the Faculty Leave during the 2018 Fall semester.

■ REFERENCES

(1) http://www.un.org/en/sections/issues-depth/water/ (accessed January 8, 2019).

(2) https://www.who.int/news-room/detail/12-07-2017-2-1-billion-people-lack-safe-drinking-water-at-home-more-than-twice-as-many-lack-safe-sanitation (accessed January 8, 2019).

(3) Nys, C.; Versieren, L.; Cordery, K. I.; Blust, R.; Smolders, E.; De Schamphelaere, K. A. Systematic evaluation of chronic metal mixture toxicity to three species and implications for risk assessment. *Environ. Sci. Technol.* **2017**, *51* (8), 4615−462.

(4) Chebeir, M.; Liu, H. Kinetics and mechanisms of Cr(VI) formation via the oxidation of Cr(III) solid phases by chlorine in drinking water. *Environ. Sci. Technol.* **2016**, *50* (2), 701−710.

(5) National Antimicrobial Resistance Monitoring System for Enteric Bacteria (NARMS). https://www.cdc.gov/narms/index.html (accessed Dec 11, 2018).

(6) Drug-resistant 'nightmare bacteria' pose growing threat: CDC, https://nypost.com/2018/04/03/drug-resistant-nightmare-bacteria-pose-growing-threat-cdc (accessed August 12, 2018).

(7) Wuijts, S.; van den Berg, H. H. J. L.; Miller, J.; Abebe, L.; Sobsey, M.; Andremont, A.; Medlicott, K. O.; Van Passel, M. W. J.; de Roda Husman, A. M. Towards a Research Agenda for Water, Sanitation, and Antimicrobial Resistance. *J. Water Health* **2017**, *15* (2), 175−184.

(8) Zhu, Y.-G.; Zhao, Y.; Li, B.; Huang, C.-L.; Zhang, S.-Y.; Chen, Y. S.; Zhang, T.; Gillings, M. R.; Su, J.-Q. Continental-Scale Pollution of Estuaries with Antibiotic Resistance Genes. *Nat. Microbiol.* **2017**, *2*, 16270.

(9) Baym, M.; Stone, L. K.; Kishony, R. Multidrug Evolutionary Strategies to Reverse Antibiotic Resistance. *Science* **2016**, *351* (6268), 40−46.

(10) Kavanagh, K. T.; Abusalem, S.; Calde-Ron, L. E. The incidence of MRSA infections in the United States: is a more comprehensive tracking system needed? *Antimicrob. Resist. Infect. Control* **2017**, *6*, 34.

(11) Vangara, A.; Pramanik, A.; Gao, Y.; Gates, K.; Begum, S.; Chandra Ray, P. Fluorescence Resonance Energy Transfer Based Highly Efficient Theranostic Nanoplatform for Two-Photon Bioimaging and Two-Photon Excited Photodynamic Therapy of Multiple Drug Resistance Bacteria. *ACS Appl. Biomater.* **2018**, *1*, 298−309.

(12) Begum, S.; Pramanik, A.; Gates, K.; Gao, Y.; Ray, P. C. Antimicrobial Peptide-Conjugated MoS2-Based Nanoplatform for Multimodal Synergistic Inactivation of Superbugs. *ACS Appl. Bio Mater.* **2019**, *2*, 769.

(13) Pramanik, A.; Jones, S.; Pedraza, F.; Vangara, A.; Sweet, C.; Williams, M. S.; Ruppa-Kasani, V.; Risher, S. E.; Sardar, D.; Ray, P. C. Fluorescent, Magnetic Multi-functional Carbon Dots for Selective Separation, Identification, and Eradication of Drug-Resistant Superbugs. *ACS Omega* **2017**, *2*, 554−562.

(14) Lee, H.; Dellatore, S. M.; Miller, W. M.; Messersmith, P. B. Mussel-inspired Surface Chemistry for Multifunctional Coatings[J]. *Science* **2007**, *318* (5849), 426−430.

(15) Waite, J. H. Mussel adhesion - essential footwork. *J. Exp. Biol.* **2017**, *220* (4), 517−530.

(16) Lee, H.; Rho, J.; Messersmith, P. B. Facile Conjugation of Biomolecules onto Surfaces *via* Mussel Adhesive Protein Inspired Coatings. *Adv. Mater.* **2009**, *21*, 431−434.

(17) Liu, Y.; Ai, K.; Lu, L. Polydopamine and Its Derivative Materials: Synthesis and Promising Applications in Energy, Environmental, and Biomedical Fields. *Chem. Rev.* **2014**, *114* (9), 5057−5115.

(18) Ryu, J. H.; Messersmith, P. B.; Lee, H. Polydopamine Surface Chemistry: A Decade of Discovery[J]. *ACS Appl. Mater. Interfaces* **2018**, *10* (9), 7523−7540.

(19) Liu, M.; Wang, S. T.; Jiang, L. Nature-Inspired Superwettability Systems. *Nat. Rev. Mater.* **2017**, *2*, 17036−17044.

(20) Zhao, D.; Kim, J. F.; Ignacz, G.; Pogany, P.; Lee, Y. M.; Szekely, G. Bio-Inspired Robust Membranes Nanoengineered from Interpenetrating Polymer Networks of Polybenzimidazole/Polydopamine. *ACS Nano* **2019**, *13*, 125−133.

(21) North, M. A.; Del Grosso, C. A.; Wilker, J. J. High strength underwater bonding with polymer mimics of mussel adhesive proteins. *ACS Appl. Mater. Interfaces* **2017**, *9* (8), 7866−7872.

(22) Ahn, B. K. Perspectives on mussel-inspired wet adhesion. *J. Am. Chem. Soc.* **2017**, *139* (30), 10166−10171.

(23) Zhang, C.; Lv, Y.; Qiu, W.-Z.; He, A.; Xu, Z.-K. Polydopamine Coatings with Nanopores for Versatile Molecular Separation. *ACS Appl. Mater. Interfaces* **2017**, *9*, 14437−1444.

(24) Han, L. B.; Gong, L.; Chen, J. S.; Zhang, J. W.; Xiang, L.; Zhang, L.; Wang, Q.; Yan, B.; Zeng, H. B. Universal Mussel-Inspired Ultrastable Surface-Anchoring Strategy *via* Adaptive Synergy of Catechol and Cations. *ACS Appl. Mater. Interfaces* **2018**, *10*, 2166−2173.

(25) Yang, H.-C.; Waldman, R. Z.; Wu, M.-B.; Hou, J.; Chen, L.; Darling, S. B.; Xu, Z.-K. Dopamine: Just the Right Medicine for Membranes. *Adv. Funct. Mater.* **2018**, *28*, 1705327.

(26) Zhao, Y. H.; Wu, Y.; Wang, L.; Zhang, M. M.; Chen, X.; Liu, M. J.; Fan, J.; Liu, J. Q.; Zhou, F.; Wang, Z. K. Bio-Inspired Reversible Underwater Adhesive. *Nat. Commun.* **2017**, *8*, 2218.

(27) Xu, Y.; You, F.; Sun, H.; Shao, L. Realizing Mussel-Inspired Polydopamine Selective Layer with Strong Solvent Resistance in Nanofiltration toward Sustainable Reclamation. *ACS Sustainable Chem. Eng.* **2017**, *5*, 5520−5528.

(28) Ma, Y. F.; Ma, S. H.; Wu, Y.; Pei, X. W.; Gorb, S. N.; Wang, Z. K.; Liu, W. M.; Zhou, F. Remote Control over Underwater Dynamic Attachment/Detachment and Locomotion. *Adv. Mater.* **2018**, *30*, 1801595.

(29) Celebi, K.; Buchheim, J.; Wyss, R. M.; Droudian, A.; Gasser, P.; Shorubalko, I.; Kye, J.-I.; Lee, C.; Park, H. G. Ultimate Permeation Across Atomically Thin Porous Graphene. *Science* **2014**, *344*, 289−292.

(30) Hu, S.; Lozada-Hidalgo, M.; Wang, F. C.; Mishchenko, A.; Schedin, F.; Nair, R. R.; Hill, E. W.; Boukhvalov, D. W.; Katsnelson, M. I.; Dryfe, R. A.; et al. Proton Transport Through One-Atom-Thick Crystals. *Nature* **2014**, *516*, 227−230.

(31) Surwade, S. P.; Smirnov, S. N.; Vlassiouk, I. V.; Unocic, R. R.; Veith, G. M.; Dai, S.; Mahurin, S. M. Water Desalination Using Nanoporous Single-Layer Graphene. *Nat. Nanotechnol.* **2015**, *10*, 459−464.

(32) Wang, L.; Boutilier, M. S. H. B.; Kidambi, P. R.; Jang, D.; Hadjiconstantinou, N. G.; Karnik, R. Fundamental Transport Mechanisms, Fabrication and Potential Applications of Nanoporous Atomically Thin Membrane. *Nat. Nanotechnol.* **2017**, *12*, 509−522.

(33) Walker, M. I.; Ubych, K.; Saraswat, V.; Chalklen, E. A.; Braeuninger-Weimer, P.; Caneva, S.; Weatherup, R. S.; Hofmann, S.; Keyser, U. F. Extrinsic Cation Selectivity of 2D Membranes. *ACS Nano* **2017**, *11*, 1340−1346.

(34) Esfandiar, A.; Radha, B.; Wang, F. C.; Yang, Q.; Hu, S.; Garaj, S.; Nair, R. R.; Geim, A. K.; Gopinadhan, K. Size Effect in Ion Transport Through Angstrom-Scale Silts. *Science* **2017**, *358*, 511−513.

(35) Alvarez, P. J. J.; Chan, C. K.; Elimelech, M.; Halas, N. J.; Villagrán, D. Emerging Opportunities for Nanotechnology to Enhance Water Security. *Nat. Nanotechnol.* **2018**, *13*, 634−641.

(36) Jones, S.; Pramanik, A.; Kanchanapally, R.; Viraka Nellore, B. P.; Begum, S.; Sweet, C.; Ray, P. C. Multifunctional Three-Dimensional Chitosan/Gold Nanoparticle/Graphene Oxide Architecture for Separation, Label-Free SERS Identification of Pharmaceutical Con-

DOI: 10.1021/acsanm.9b00161
ACS Appl. Nano Mater. XXXX, XXX, XXX−XXX

taminants, and Effective Killing of Superbugs. *ACS Sustainable Chem. Eng.* **2017**, *5*, 7175−7187.

(37) Jones, S.; Sinha, S. S.; Pramanik, A.; Ray, P. C. Three-dimensional (3D) plasmonic hot spots for label-free sensing and effective photothermal killing of multiple drug resistant superbugs. *Nanoscale* **2016**, *8*, 18301−18308.

(38) Viraka Nellore, B. P.; Kanchanapally, R.; Pedraza, F.; Sinha, S. S.; Pramanik, A.; Hamme, A. T.; Arslan, Z.; Sardar, D.; Ray, P. C. Bio-Conjugated CNT-Bridged 3D Porous Graphene Oxide Membrane for Highly Efficient Disinfection of Pathogenic Bacteria and Removal of Toxic Metals from Water. *ACS Appl. Mater. Interfaces* **2015**, *7*, 19210−19218.

(39) Pramanik, A.; Jones, S.; Gao, Y.; Sweet, C.; Begum, S.; Shukla, M. K.; Bu-Chanan, J. P.; Moser, R. D.; Ray, P. C. A bio-conjugated chitosan wrapped CNT based 3D nanoporous architect re for separa-tion and inactivation of Rotavirus and Shigell a waterborne pathogens. *J. Mater. Chem. B* **2017**, *5* (48), 9522−9531.

(40) Mao, C. Y.; Xiang, Y. M.; Liu, X. M.; Cui, Z. D.; Yang, X. J.; Yeung, K. W. K.; Pan, H. B.; Wang, X. B.; Chu, P. K.; Wu, S. L. Photo-Inspired Antimicrobial Activity and Wound Healing Acceleration by Hydrogel Embedded with Ag/Ag@AgCl/ZnO Nanostructures. *ACS Nano* **2017**, *11*, 9010−9021.

(41) Liu, S.; Zeng, T. H.; Hofmann, M.; Burcombe, E.; Wei, J.; Jiang, R.; Kong, J.; Chen, Y. An tibacterial Activity of Graphite, Graphite Oxide, Graphene Oxide, and Reduced Graphene Oxide: Membrane and Oxidative Stress. *ACS Nano* **2011**, *5*, 6971−6980.

(42) Zou, X.; Zhang, L.; Wang, Z.; Luo, Y. Mechanisms of the Antimicrobial Activities of Graphene Materials. *J. Am. Chem. Soc.* **2016**, *138*, 2064−2077.

(43) Reuter, M.; Schwieger, C.; Meister, A.; Karlsson, G.; Blume, A. Poly-L-Lysines and Poly-L-Arginines Induce Leakage of Negatively Charged Phospholipid Vesicles and Translocate through the Lipid Bilayer upon Electrostatic Binding to the Membrane. *Biophys. Chem.* **2009**, *144*, 27−37.

(44) Hyldgaard, M.; Mygind, T.; Vad, B. S.; Stenvang, M.; Otzen, D. E.; Meyer, R. L. The Antimicrobial Mechanism of Action of Epsilon-Poly-L-Lysine. *Appl. Environ. Microbiol.* **2014**, *80*, 7758−7770.

(45) Ushimaru, K.; Hamano, Y.; Katano, H. Antimicrobial activity of ε-poly-L-lysine after forming a water-insoluble complex with an anionic surfactant. *Biomacromolecules* **2017**, *18*, 1387−1392.

DOI: 10.1021/acsanm.9b00161
ACS Appl. Nano Mater. XXXX, XXX, XXX−XXX